Middle-East Journal of Scientific Research 24 (4): 1551-1557, 2016
ISSN 1990-9233

DOI: 10.5829/idosi.mejsr.2016.24.04.23387

Rotation Invariant Texture Analysis of Lung Tumor CT Images Using Radon Transform

G.V. Jason Jebasingh, B. Suresh Chander Kapali, B. Priyanka and A. Brightline

Department of Biomedical Engineering, Alpha College of Engineering, Chennai, India

Abstract: Texture analysis is an important area of study in image processing. It is a key problem in many application areas, including medical imaging, remote sensing, object recognition and so forth However, the problem with the majority of existing works on texture analysis is that it is assumed that all images are acquired from the same orientation. This assumption is not realistic in practical applications, where images may be taken with different rotation, scale, etc. As a result, the performance of these methods becomes worse when this underlying assumption is no longer valid. This paper deals with the rotation invariant texture analysis for which initially the CT image is taken and texture category is found out. The images are categorized by the above under individual groups, Isotropic, Anisotropic or mixed. The peak obtained from the plot of variance and theta determines this. The feature values for the CT image are thus found out.

Key words: Invariant · Texture · Radon transforms and anisotropic

INTRODUCTION

In this paper a new scheme for texture analysis is carried out in this the texture category is found out by applying Radon transform. here the image taken for analysis is CT image of lung. CT imaging is one of the best tools for studying the chest and abdomen because it provides detailed, cross-sectional views of all types of tissue. often the preferred method for diagnosing many different cancers [1], including lung, liver and pancreatic cancer, since the image allows a physician to confirm the presence of a tumor and measure its size [2], precise location and the extent of the tumor's involvement with other nearby tissue. invaluable in diagnosing and treating spinal problems and injuries to the hands, feet and other skeletal structures because it can clearly show even very small bones as well as surrounding tissues such as muscle and blood vessels [3, 4]. Radon transform is calculated for the CT image and variance is found for the obtained angle a graph is plot between variance and theta that determines the category of the image. Texture feature extraction is carried out by Gabor wavelet transform; here the feature vectors were obtained. Feature vectors were calculated for test images [5].

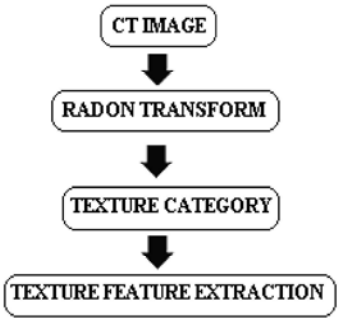

Fig. 1: Block diagram.

Texture Category

Radon Transform: The Radon transform is the projection of the image intensity along a radial line oriented at a specific angle [6]. It transforms a 2D image with lines (line-trends) into a domain of the possible line parameters ρ and θ, where ρ is the smallest distance from the origin and θ is its angle with the x-axis. The Radon transform is defined as

$$R(\rho,\theta) = \int_{-\infty}^{+\infty}\int_{-\infty}^{+\infty} f(x,y)\delta(\rho - x\cos\theta - y\sin\theta)dxdy, \quad (1)$$

Corresponding Author: B. Suresh Chander Kapali, Department of Biomedical Engineering, Alpha College of Engineering, Chennai, India.

Or Equivalently:

$$R(\rho,\theta) = \int_{-\infty}^{+\infty} f(\rho\cos\theta - s\sin\theta, \rho\sin\theta + s\cos\theta)ds, \quad (2)$$

The Radon transform is applied for CT image for angle 0° to 179°. From the out put obtained the variance is calculated for all the possible degrees obtained. A histogram is obtained by taking angle along X-axis and variance along Y-axis [7]. The wave form in the histogram represents the number of peaks which tells about the texture category, if the number of peaks is more than 7 then it belongs to category called mixed and number of peaks less than 7 it belongs to category Isotropic and with one peak represent Anisotropic [8].

Slice Reconstruction: The Radon transform of an image represented by the function f(x,y) can be defined as a series of line integrals through f(x,y) at different offsets from the origin. This is defined mathematically as:

$$R(P, \tau) = \int_{-\infty}^{\infty} f(x, px + \tau)\, dx \quad (4)$$

where p and tau are the slope and intercepts of the line.

A more directly applicable form of the transform can be defined by using a delta function: 8 8

$$R(r, \theta) = \int_{-\infty}^{\infty}\int_{-\infty}^{\infty} f(x, y)\, \delta(x\cos\theta + y\sin\theta - r)\, dxdy \quad (5)$$

where theta is the angle of the line and r is the perpendicular offset of the line.

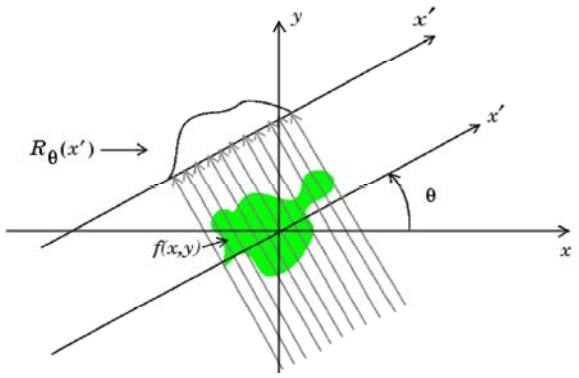

Fig. 3.1: Radon transform

The acquisition of data in medical imaging techniques such as MRI, CT and PET scanners involves a similar method of projecting a beam through an object and the data is in a similar form to that described in the second equation above. The plot of the Radon transform, or scanner data, is referred to as a sinogram due to its characteristic sinusoid shape. Figure 3.2 shows a simple non-homogeneous shape and the sinogram created by taking the Radon transform at intervals of one degree from 0 to 180 degrees [9].

Texture Feature Extraction

Segmentation- Level Set Contour Method: In image segmentation, active contours are dynamic curves that move toward the object boundaries. To achieve this goal [10], we explicitly define an external energy that can move the zero level curves toward the object boundaries. Let I be an image and g be the edge indicator function defined by

$$g = \frac{1}{1+|\Delta G\sigma * I|^2}$$

where Gσ is the Gaussian kernel with standard deviation σ. We define an external energy for a function φ(x, y) as below

$$\epsilon_{g,\lambda,\nu}(\varphi) = \lambda\, Lg(\varphi) + \nu\, Ag(\varphi) \quad (9)$$

where λ > 0 and ν are constants and the terms Lg(φ) and Ag(C) are defined by

$$Lg(\varphi) = \int_\Omega g\delta(\varphi)\left|\nabla\varphi\right| dxdy| \quad (10)$$

And

$$Ag(\varphi) = \int_\Omega gH(-\varphi)dxdy \quad (11)$$

respectively, where δ is the univariate Dirac function and H is the Heaviside function. Now, we define the following total energy functional

$$\epsilon(\varphi) = \mu P(\varphi) + \epsilon_{g,\lambda,\nu}(\varphi) \quad (12)$$

The external energy $\epsilon_{g,\lambda,\nu}$ drives the zero level set toward the object boundaries, while the internal energy μP(φ) penalizes the deviation of φ from a signed distance function during its evolution.

To understand the geometric meaning of the energy Lg(φ), we suppose that the zero level set of φ can be represented by a differentiable parameterized curve C(p), p ∈ [0, 1]. It is well known that the energy functional Lg(φ) computes the length of the zero level curve of φ in the conformal metric ds = g(C(p))|C'(p)|dp. The energy functional Ag(φ) is introduced to speed up curve evolution. Note that, when the function g is constant 1, the energy functional in the area of the region Ω_φ = {(x, y)|φ(x, y) < 0}. The energy functional Ag(φ) can be viewed as the weighted area of Ω_φ. The coefficient ν of Ag can be positive or negative, depending on the relative position of the initial contour to the object of interest. For example, if the initial contours are placed outside the object [11], the coefficient ν in the weighted area term should take positive value, so that the contours can shrink faster. If the initial contours are placed inside the object, the coefficient ν should take negative value to speed up the expansion of the contours [12].

By calculus of variations, the Gateaux derivative (first variation) of the functional ϵ can be written as

$$\frac{\partial \epsilon}{\partial \varphi} = -\mu[\Delta\varphi - \mathrm{div}(\frac{\Delta\varphi}{|\Delta\varphi|})] - \lambda\delta(\varphi)\mathrm{div}(g\frac{\Delta\varphi}{|\Delta\varphi|}) - \nu g\delta(\varphi)$$

where Δ is the Laplacian operator. Therefore, the function φ that minimizes this functional satisfies the Euler-Lagrange equation $\partial\epsilon/\partial\varphi = 0$. The steepest descent process for minimization of the functional ϵ is the following gradient flow:

$$\frac{\partial \varphi}{\partial t} = \mu[\Delta\varphi - \mathrm{div}(\frac{\Delta\varphi}{|\Delta\varphi|})] + \lambda\delta(\varphi)\mathrm{div}(g\frac{\Delta\varphi}{|\Delta\varphi|}) + \nu g\delta(\varphi) \quad (13)$$

This gradient flow is the evolution equation of the level set function in the proposed method [13].

The second and the third term in the right hand side correspond to the gradient flows of the energy functional λLg(φ) and νAg(φ), respectively and are responsible of driving the zero level curve towards the object boundaries. To explain the effect of the first term, which is associated to the internal energy μP(φ), we notice that the gradient flow

$$\Delta\varphi = \mathrm{div}(\frac{\Delta\varphi}{|\Delta\varphi|} = \mathrm{div}[(1-\frac{1}{|\Delta\varphi|})\Delta\varphi]$$

has the factor (1 - 1/|Δφ|) as diffusion rate. If |Δφ| > 1, the diffusion rate is positive and the effect of this term is the usual diffusion, i.e. making φ more even and therefore reduce the gradient |Δφ|. If |Δφ| < 1, the term has effect of reverse diffusion and therefore increase the gradient [14].

Gabor Wavelet Transform: The texture feature extraction is carried out using Gabor wavelet transform [15, 16]. A 2D Gabor function $g(x, y)$ and its Fourier transform is defined as

$$+ j2\pi Wx\Big| \quad (3)$$

$$G(u,v) = \exp\left[-\frac{1}{2}\left(\frac{(u-W)^2}{\sigma_u} + \frac{v^2}{\sigma_v}\right)\right] \quad (4)$$

where. $\sigma_u = 1/2\pi\,\sigma_x$ and $\sigma_v = 1/2\pi\,\sigma_y|$. Considering $g(x, y)$ as the mother Gabor wavelet, a class of self-similar functions (filters) [17], referred to as discrete Gabor wavelets can be obtained by appropriate dilations and rotations of $g(x, y)$ as;

$$g_{mn}(x,y) = a^{-m}g(x',y'), \quad \text{a>1, m,n=integer.}$$

$$x' = a^{-m}(x\cos\beta + y\sin\beta),$$
$$y' = a^{-m}(-x\sin\beta + y\cos\beta). \quad (5)$$

Here, we define the parameters of the Gabor filters as;

$$a = \left(\frac{U_k}{U_l}\right)^{\frac{1}{S-1}} \quad \beta = \frac{n\pi}{K}$$

$$\sigma_u = \frac{(a-1)U_k}{(a+1)\sqrt{2\ln 2}}$$

$$\sigma_v = \tan\left(\frac{\pi}{2k}\right)\left[U_k - 2\ln\left(\frac{2\sigma_u^2}{U_k}\right)\right]$$

$$\times\left[2\ln 2 - \left(\frac{(2\ln 2)^2\sigma_u^2}{U_k}\right)\right] \quad (6)$$

where S and K are the number of scales and orientations and Ul and Uh denote the lower and upper center frequencies [18]. Given an image $I(x, y)$, its Gabor wavelet transform is then defined as;

$$G_{mn}(x,y) = \int\int I(s,t)g_{mn}^*(x-s, y-t)dsdt \quad (7)$$

We can construct a texture feature vector *ft* for *S* scales and *K* orientations using the means and standard deviations.

RESULTS

In this work the feature extraction of CT slice of lung image is preceded with the proposed technique. Fig.6.1 shows the original CT slice of lung image.

Fig. 6.1: CT slice of Lung image with starting stage of Tumor.

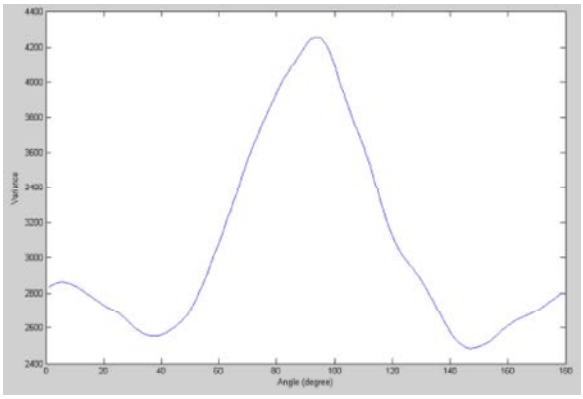

Fig. 6.2: Histogram representing Anisotropic having no. of peaks = 1.

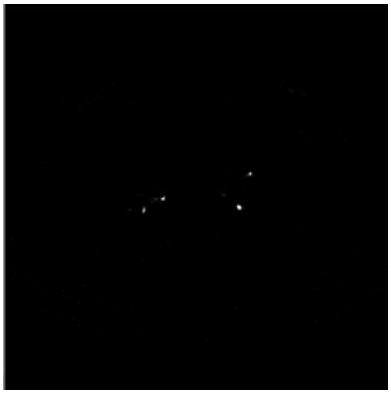

Fig. 6.3: segmented CT slice of lung image.

The feature values are calculated by using Gabor filter. the Gabor filter is set for 4 scales and 4 orientations. For each feature there will be 16 values. Here we are finding feature values for mean, standard deviation, Energy and Entropy.

Table 6.1: Represents the feature values of CT slice of lung image.

Scale and Orientation	Mean	Standard Deviation	Energy	Entropy
			---------1.0e+003 *---------	
[1,1]	0.0032	0.0164	0.0737	4.6623
[1,2]	0.0019	0.0052	0.0160	3.3442
[1,3]	0.0033	0.0002	0.0744	4.8631
[1,4]	0.0020	0.0053	0.0161	3.3426
[2,1]	0.0020	0.0127	0.0457	2.4089
[2,2]	0.0014	0.0041	0.0110	2.1979
[2,3]	0.0021	0.0004	0.0452	2.5787
[2,4]	0.0014	0.0041	0.0112	2.2056
[3,1]	0.0021	0.0088	0.0244	2.9130
[3,2]	0.0015	0.0028	0.0072	2.5952
[3,3]	0.0021	0.0006	0.0236	3.0679
[3,4]	0.0015	0.0028	0.0071	2.6239
[4,1]	0.0021	0.0061	0.0122	3.4851
[4,2]	0.0015	0.0019	0.0038	2.9527
[4,3]	0.0022	0.0006	0.0126	3.6532
[4,4]	0.0015	0.0019	0.0038	3.0102

[1,1] Represents scale 1 and orientation 1.similary [1, 2] represents scale 1 and orientation 2.[4,4] represents scale 4 and orientation 4.

These were the texture features calculated for CT lung image with starting stage of tumor which comes under the category Anisotropic. With this another CT lung image is compared which belongs to the same category.

Fig. 6.4: CT slice of lung image with tumor.

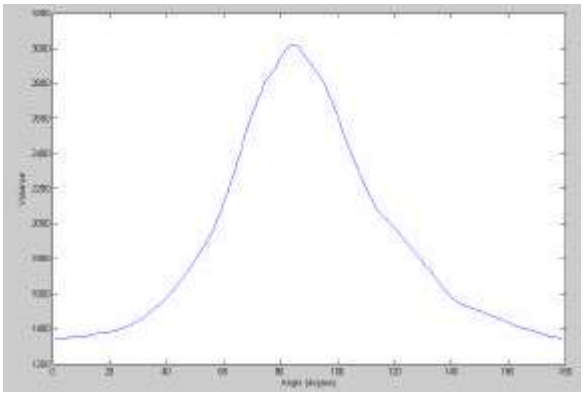

Fig. 6.5: Histogram representing Anisotropic having no. of peaks = 1.

Fig. 6.6: Segmented CT slice of lung image.

The feature values were calculated using Gabor filter for 4 scales and 4 orientations. This image belongs to the category Anisotropic.

Table 6.2: Represents the feature values for CT slice of lung image with tumor

Scale and Orientation	Mean	Standard Deviation	Energy --------1.0e+003 *---------	Entropy
[1,1]	0.0033	0.0164	0.0748	4.7034
[1,2]	0.0012	0.0053	0.0098	2.1396
[1,3]	0.0002	0.0005	0.0017	0.4101
[1,4]	0.0012	0.0053	0.0098	2.1671
[2,1]	0.0021	0.0127	0.0464	2.3043
[2,2]	0.0009	0.0041	0.0080	1.2455
[2,3]	0.0003	0.0007	0.0033	0.4962
[2,4]	0.0009	0.0042	0.0088	1.3280
[3,1]	0.0021	0.0088	0.0244	2.7543
[3,2]	0.0009	0.0029	0.0052	1.5138
[3,3]	0.0005	0.0009	0.0039	0.7291
[3,4]	0.0011	0.0030	0.0077	1.6755
[4,1]	0.0022	0.0061	0.0127	3.3933
[4,2]	0.0010	0.0020	0.0029	1.8218
[4,3]	0.0006	0.0009	0.0029	0.9495
[4,4]	0.0011	0.0021	0.0041	1.9926

The feature values for the two CT images belong to the same category were found out and tabulated. We keep this as class I.

Similarly we can find the texture feature values for all the images belongs to the same category and we can compare with the slightly tumor affected image.

Now we can discuss the same procedure for another category image. Figure 6.7 shows the CT slice of lung image with starting stage of tumor.

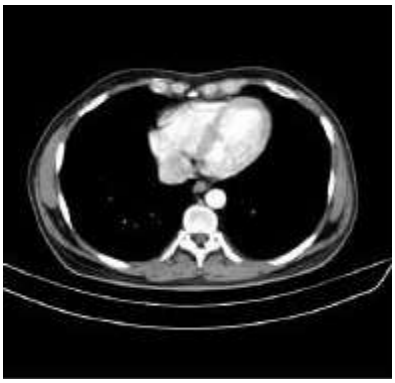

Fig. 6.7: CT slice of Lung image with starting stage of Tumor.

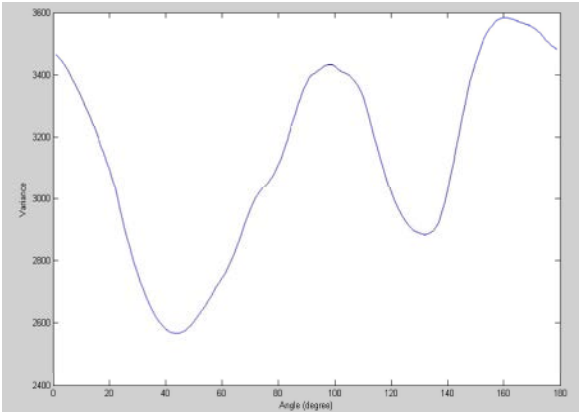

Fig. 6.8: Histogram representing isotropic having no. of peaks = 2.

Fig. 6.9: Segmented CT slice of lung image.

Table 6.3: Represents the feature values for CT slice of lung image with starting stage of tumor.

Scale and Orientation	Mean	Standard Deviation	Energy --------1.0e+003 *---------	Entropy
-[1,1]	0.0002	0.0002	0.0006	0.5199
[1,2]	0.0012	0.0002	0.0082	2.1732
[1,3]	0.0033	0.0002	0.0738	4.7481
[1,4]	0.0012	0.0002	0.0083	2.1799
[2,1]	0.0003	0.0003	0.0016	0.6701
[2,2]	0.0008	0.0003	0.0058	1.4533
[2,3]	0.0021	0.0003	0.0447	2.5317
[2,4]	0.0009	0.0003	0.0061	1.4587
[3,1]	0.0004	0.0003	0.0013	0.8273
[3,2]	0.0009	0.0004	0.0034	1.7431
[3,3]	0.0021	0.0004	0.0223	3.0149
[3,4]	0.0009	0.0004	0.0035	1.7464
[4,1]	0.0004	0.0003	0.0005	0.9164
[4,2]	0.0009	0.0004	0.0017	1.9850
[4,3]	0.0021	0.0003	0.0114	3.5219
[4,4]	0.0009	0.0003	0.0016	1.9633

The above table represents the feature values of the CT slice of lung image with starting stage of tumor for the category Isotropic. Similarly the feature value is calculated for another Isotropic image with tumor.

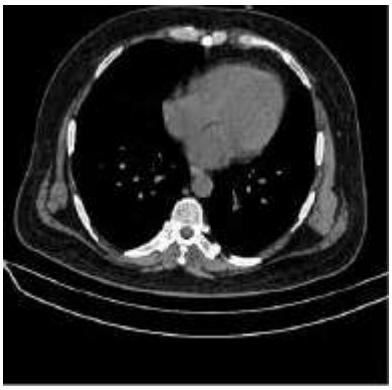

Fig. 6.10: CT slice of lung image with tumor.

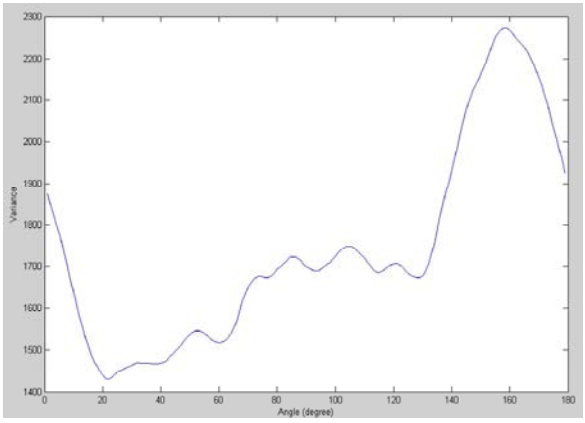

Fig. 6.11: Histogram representing isotropic having no. of peaks = 6.

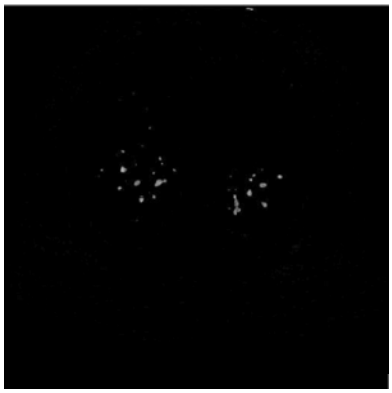

Fig. 6.12: Segmented CT slice of lung image.

Table 6.3: Represents the feature values for CT slice of lung image with tumor for Isotropic

Scale and Orientation	Mean	Standard Deviation	Energy --------1.0e+003 *--------	Entropy
[1,1]	0.0035	0.0163	0.0751	5.0450
[1,2]	0.0022	0.0052	0.0175	3.6967
[1,3]	0.0035	0.0005	0.0755	5.0721
[1,4]	0.0022	0.0052	0.0173	3.6944
[2,1]	0.0026	0.0127	0.0488	3.2849
[2,2]	0.0019	0.0041	0.0144	3.0014
[2,3]	0.0026	0.0009	0.0491	3.3277
[2,4]	0.0019	0.0041	0.0139	2.9999
[3,1]	0.0029	0.0088	0.0304	4.1575
[3,2]	0.0022	0.0029	0.0120	3.7088
[3,3]	0.0028	0.0013	0.0290	4.1149
[3,4]	0.0022	0.0029	0.0133	3.7664
[4,1]	0.0030	0.0060	0.0179	4.8170
[4,2]	0.0023	0.0021	0.0087	4.1432
[4,3]	0.0029	0.0014	0.0173	4.7862
[4,4]	0.0023	0.0021	0.0089	4.2256

The feature values for the two CT slice of lung images belong to the same category Isotropic were found out and tabulated. We keep this as class II.

Similarly the feature values for discrete radon transform should be find out and classification should be made for both and from the distance obtained future analysis can be made.

CONCLUTION

The feature values for different category classes Isotropic and Anisotropic were found and the feature values were displayed in tables above. Similarly the feature values for the original image should be find out and classification should be performed and from that diagnosis should be made.

REFERENCES

1. Cai-Xia Deng, Zuo-Xian Fu and Xiao-Jian Ma, 2007. The Properties of Gabor Wavelet Transform, Proceedings of the 2007 International Conference on Wavelet Analysis and Pattern Recognition, Beijing, China, pp: 2-4.
2. Gang Zhang and Zong-Min Ma, 2007. Texture Feature Extraction and Description Using Gabor Wavelet in Content-Based Medical Image Retrieval, Proceedings of the 2007 International Conference on Wavelet Analysis and Pattern Recognition, Beijing, China, pp: 2-4.
3. Kourosh Jafari-Khouzani and Hamid Soltanian-Zadeh, 2005. Radon Transform Orientation Estimation for Rotation Invariant Texture Analysis, IEEE Transactions on Pattern Analysis and Machine Intelligence, 27(6).
4. Manjunath, B.S. and W.Y. Ma, 1996. Texture features for browsing and retrival of image data, IEEE Transactions on Pattern Analysis and Machine Intelligence, pp: 18.
5. Thomas L. Marzetta and Larry A. Shepp, 1999. A surprising Radon transform result and its application to motion detection, IEEE Transactions on Image Processing, 8(8).
6. Wook-jin choi, *et al*, XXXX. Automated pulmonary nodule detection in computed tomography images: A hierarchical block classification approach.
7. Khin Mya Mya Tun, *et al*., 2014. Feature extraction and classification of lung cancer nodule detection using image processing technique, International Journal of Engineering and Technology (IJERT), 3(3).
8. Jaspinder kaur, *et al*., 2014. An automatic CAD system for early detection of lung tumor using back propogation network, International conference on medical imaging,m-health and emerging communication system (Medcom), pp: 257-261.
9. Hamid bhagerish, *et al*., XXXX. Mass detection in lung CT images using region growing sementation and decision making based on fuzzy systems, I.J Image.graphic and signal processing.
10. Prashant Naresh *et al*., 2014. Image processing and classification techniques for early detection of lung cancer for preventive health care:A survey, International Journal of Recent Trends in Engineering & Technology, 11: 595-601.
11. Taruna aggarwal, *et al*., 2015. Feature extraction and LDA based classification of lung nodules in chest CT scan images, International conference on advances in computing,communication and informatics (ICACCI), pp: 1189-1193.
12. Farzad vasheghani farahani, *et al*., 2015. Lung nodule diagnosis from CT images based on Ensemble learning, International conference on Computational intelligence in Bioinformatics and computational biology (CIBCB), pp: 1-7,12-15.
13. Rithika aggarwal, *et al*., 2015. Detection of lung cancer using content based medical iamge retrieval, Fifth International conference on Advanced Computing & Communication Technologies, pp: 48-52.
14. Bhagyashri G. Patil, *et al* "Cancer cells detection using digital image processing methods" International journal of latest trends in engineering & technology(IJLTET),vol.3 isssue 4, pp.45-49 4th March 2014.
15. H.mahersia, *et al*., 2015. Lung cancer detection on CT scan images:A review on the analysis technique, International Journal of Advanced Research in Artificial Intelligence, 4(4): 36-46.
16. Delogu, P., *et al*, XXXX. Pre-processing methods for nodule detection in lung CT.
17. Vaibhav K. Lithitkar, *et al* 2014. Automated detection on cancerous lung nodule from the computed tomography images, IOSR Journal of Computer Engineering (IOSR-JCE), 16(1): 5-11.
18. Amjed S. Al-fahoum, *et al*, 2014. Automated detection of lung cancer using statistical and morphological image processing technique, Journal of Biomedical Graphics and Computing, 4(2): 33-42.